HHS Public Access

Author manuscript

Dev Biol. Author manuscript; available in PMC 2022 February 01.

Published in final edited form as:

Dev Biol. 2021 February ; 470: 136–146. doi:10.1016/j.ydbio.2020.11.004.

Dysregulated BMP signaling through ACVR1 impairs digit joint development in fibrodysplasia ossificans progressiva (FOP)

O. Will Towler[1,4], **Sun H. Peck**[*,1,4], **Frederick S. Kaplan**[1,2,4], **Eileen M. Shore**[1,3,4]

[1]Department of Orthopaedic Surgery, Perelman School of Medicine, University of Pennsylvania, 3450 Hamilton Walk, 309A Stemmler Hall, Philadelphia, PA 19104.

[2]Department of Medicine, Perelman School of Medicine, University of Pennsylvania, 3450 Hamilton Walk, 309A Stemmler Hall, Philadelphia, PA 19104.

[3]Department of Genetics, Perelman School of Medicine, University of Pennsylvania, 3450 Hamilton Walk, 309A Stemmler Hall, Philadelphia, PA 19104.

[4]Center for Research in FOP & Related Disorders, Perelman School of Medicine, University of Pennsylvania, 3450 Hamilton Walk, 309A Stemmler Hall, Philadelphia, PA 19104.

Abstract

The development of joints in the mammalian skeleton depends on the precise regulation of multiple interacting signaling pathways including the bone morphogenetic protein (BMP) pathway, a key regulator of joint development, digit patterning, skeletal growth, and chondrogenesis. Mutations in the BMP receptor *ACVR1* cause the rare genetic disease fibrodysplasia ossificans progressiva (FOP) in which extensive and progressive extra-skeletal bone forms in soft connective tissues after birth. These mutations, which enhance BMP-pSmad1/5 pathway activity to induce ectopic bone, also affect skeletal development. FOP can be diagnosed at birth by symmetric, characteristic malformations of the great toes (first digits) that are associated with decreased joint mobility, shortened digit length, and absent, fused, and/or malformed phalanges. To elucidate the role of ACVR1-mediated BMP signaling in digit skeletal development, we used an *Acvr1*^{R206H};*Prrx1-Cre* knock-in mouse model that mimics the first digit phenotype of human FOP. We have determined that the effects of increased Acvr1-mediated signaling by the *Acvr1*^{R206H} mutation are not limited to the first digit but alter BMP signaling, *Gdf5*+ joint progenitor cell localization, and joint development in a manner that differently affects individual digits during embryogenesis. The *Acvr1*^{R206H} mutation leads to delayed and disrupted joint specification and cleavage in the digits and alters the development of cartilage and endochondral ossification at sites of joint morphogenesis. These findings demonstrate an important role for ACVR1-mediated BMP signaling in the regulation of joint and skeletal

Corresponding author: Eileen M. Shore (shore@pennmedicine.upenn.edu).

*Current address: Division of Clinical Pharmacology and Vanderbilt Center for Bone Biology, Vanderbilt University Medical Center, 1211 Medical Center Dr., Nashville, TN, 37232

Declarations of conflicts of interest: none.

formation, show a direct link between failure to restrict BMP signaling in the digit joint interzone and failure of joint cleavage at the presumptive interzone, and implicate impaired, digit-specific joint development as the proximal cause of digit malformation in FOP.

Keywords

BMP; FOP; ACVR1; digit; joint; chondrogenesis

Introduction

The development of joints throughout the appendicular skeleton follows a general template that is combined with site-specific modifications to produce specific adult morphologies and tissues. In all mammalian joints, development proceeds via cavitation of pre-chondrogenic condensed mesenchyme to produce distinct nascent skeletal elements separated by a primordial tissue called the joint interzone (Mitrovic 1977). Cavitation and separation, or cleavage, is the direct effect of the migration, layered organization, and differentiation of cells around and within the presumptive interzone (Koyama et al 2008). Down-regulation of the bone morphogenetic protein (BMP)-pSMAD1/5 signaling pathway and expression of *Gdf5* in migrating joint progenitor cells are critical for the initiation and progression of joint formation (Storm et al 1994; Koyama et al 2007). This general process of joint formation is further influenced by joint-specific sets of gene expression and signaling in order to induce the varied joint and skeletal morphologies that permit specialized skeletal functions (Settle et al 2003; Chen et al 2016). While extensive and elegant studies have elucidated some of the interactions among these regulatory mechanisms, the full suite of molecular actors in this generation of site-specific morphology, structure, and function continues to be unraveled.

Failure to regulate the BMP pathway during embryonic development leads to a variety of skeletal phenotypes, including failure of joint cleavage and development of joint tissues (reviewed Stricker and Mundlos 2011; Singh et al 2018), syndactyly (Merino et al 1999), polydactyly (Norrie et al 2014), limb truncation (Ahn et al 2001), and generalized chondrodysplasia (Rigueur et al 2015). Related to these are the well-documented roles of BMP pathway regulation during the development of the mammalian skeleton, including joint formation (Brunet et al 1998), patterning the antero-posterior and proximo-distal morphology of the limb (reviewed in Pignatti et al 2014), and chondrogenic and osteogenic differentiation (Pizette and Niswander 2000; reviewed in Wu et al 2016). Proper joint formation within the developing skeletal elements is in part dependent on reduction and/or inhibition of pSMAD1/5 signaling downstream of activated BMP pathway receptors (Singh et al 2018). In particular, the process of joint cleavage has been linked to the local regulation of BMP pathway signaling (Ray et al 2015), Gdf5 expression (Storm et al 1994; Koyama et al 2008), and embryo movement (Singh et al 2018). In genetic mouse models of disinhibited BMP signaling, such as knockout of the BMP antagonist *Noggin* or constitutive activation of the type I BMP receptor BMPR1B, enhanced BMP pathway activity causes generalized skeletal dysplasia and entirely ablates joint formation (Brunet et al 1998; Ray et al 2015).

The type I BMP receptor ACVR1 (ALK2) has only recently received attention regarding its role in skeletal development, with absence of Acvr1 leading to mild axial and appendicular skeletal dysplasia in mouse models (Rigueur et al 2015). Deletion of *Acvr1 (Alk2)* in the limb mesenchyme leads to mild chondrogenic defects in digits 2–5; however, in digit 1, the proximal phalanx fails to ossify, and both anterior and interdigital expression of *Gdf5* is expanded (Hildebrandt et al 2019), suggesting that digit 1 is more highly dependent on Acvr1 function. Mildly activating mutations in *ACVR1* cause the disease fibrodysplasia ossificans progressiva (FOP; MIM #135100), a disabling genetic disorder characterized by progressive heterotopic (extra-skeletal) ossification (HO) (Shore et al 2006). This condition can often be clinically diagnosed in young children prior to onset of heterotopic ossification by a highly penetrant, congenital, characteristic malformation of the great toes (first digits) (Schroeder and Zasloff 1980). This digit malformation has been given little clinical attention except for noting its extremely high penetrance and thus usefulness as a diagnostic tool (Tünte et al 1967; Kaplan et al 2008).

Studies of radiographs from small cohorts of FOP patients identified distal phalangeal coalition or fusion (Schroeder and Zaslof 1980) and ectopic ossification centers distal to the first metatarsal (Harrison et al 2005), prompting our investigation of a developmental regulation of joint cleavage and interzone specification mediated by *ACVR1*. The majority of cases of FOP are caused by a recurrent *de novo ACVR1* R206H (c.617G>A) mutation (Shore et al 2006). To investigate the role of *ACVR1* R206H in malformation of digits and digital joints in detail, we used a mouse model, $Acvr1^{R206H/+}$;*Prrx1-Cre,* in which the mutation is specifically expressed in cells of the developing skeletal elements of the limbs (Chakkalakal et al 2016). These mice not only form post-natal heterotopic ossification as occurs in human FOP, but also recapitulate the characteristic FOP great toe malformations and provide an *in vivo* model to investigate the role of Acvr1 signaling in skeletal development. Using these mice, we investigated the effect of this activating mutation in *ACVR1* on site-specific joint development and morphology, focusing on the digits.

Methods

Mouse models

A conditional $Acvr1^{R206H/+}$;*Prrx1-Cre* knock-in mouse model was previously described (Hatsell et al 2015; Chakkalakal et al 2016). The ACVR1 R206H mutation occurs in most people who have fibrodysplasia ossificans progressiva (FOP). $Acvr1^{+/+}$ (with or without Cre) and $Acvr1^{R206H/+}$ (without Cre) littermates have been previously demonstrated to have no appreciable phenotype (Logan et al 2002; Chakkalakal et al 2016) and were used as controls. P14 and P28 mutants are readily phenotyped by reduced hindlimb mobility and foot morphology, whereas all control mice had no phenotype and could thus be grouped under the single label “control.” Genotype is indicated when available. All animal procedures were reviewed and approved by the Institutional Animal Care and Use Committee at the University of Pennsylvania.

Whole mount immunohistochemistry

Timed pregnant dams were sacrificed by CO_2 asphyxiation and embryos harvested and transferred to chilled PBS. Embryo age was determined by plug date, limb morphology, and cranial morphology (EMAP eMouse Atlas Project, http://www.emouseatlas.org; Richardson et al 2014). Embryos were fixed in 4% PFA at 4˚C overnight. Whole mount immunohistochemistry was carried out as described in Yokomizo et al 2012, using a pSmad1/5 primary antibody (P-Smad1/5 (S463/465)/9(S465/467), Cell Signaling 13820S) at 1:200 dilution and a goat anti-rabbit secondary antibody (Goat anti-Rabbit IgG (H+L) AlexaFluor Plus 647, Invitrogen) at 1:2000 dilution. Nuclei were stained using a 1:2000 dilution of SYTOX Orange Dead Cell Stain (ThermoFisher Scientific). Cleared samples were mounted using custom FastWells between two 1-weight glass slide coverslips and imaged with a Leica confocal microscope at 2.4 μm steps through the entire tissue. Three-dimensional images were reconstructed and rendered using Imaris software (Oxford Instruments).

Whole mount staining of cartilage and bone in adult, fetal, and neonatal mice

Skeletal tissue dissection, processing, and staining were performed by standard methods (McLeod 1980). Skeletal elements were stained with Alizarin Red S (mineralized tissue/bone; Sigma) and Alcian Blue GS (glycose-amino-glycans/cartilage; Sigma), then cleared and preserved in glycerol for imaging and analysis using an M250C Leica stereomicroscope fitted with a Leica DFC450 C camera.

Histological analysis

Samples were decalcified using formic acid (Immunocal; Fisher Scientific) for three days, or 1% EDTA for a minimum of three days for adult tissues (P14, P28) or a single day for embryonic (E14.5) tissues. Samples were processed into paraffin. Serial 5-μm sections were stained in Hubert's Modified Hematoxylin (Fisher) and acid Eosin (Azer Scientific); 1% Picrosirius red staining solution (Direct Red 80, Sigma Aldrich) and 3% Alcian Blue 8GX (Sigma Aldrich), pH2.5. Embryonic tissues were stained using Nuclear Fast Red (American Master Tech) and Alcian Blue, pH2.5. Slides were imaged with an Eclipse 90i upright microscope (Nikon) or Leica DM70 (Leica) under brightfield.

Immunohistochemistry

Tissue samples were fixed in 4% PFA overnight at 4˚C. PFA was removed by 2 washes in PBS. Limbs were dissected and dehydrated in a methanol gradient for storage at −20˚C until needed. Limbs were then rehydrated through a gradient into PBS, floated in 30% sucrose, and frozen in blocks in OCT compound (SciGen). 8 μm sections were taken at −22˚C using a cryostat microtome (Thermo Scientific) and stored at −20˚C until needed. Sections were washed, blocked in Background Buster (Innovex Biosciences), and incubated overnight with appropriate dilutions of antibodies (1:50 pSmad1/5/9, Cell Signaling; 1:200 Sox9, Abcam; 1:200 Sox6, Abcam).

Whole mount in situ hybridization

In situ hybridization of whole embryonic limbs to detect *Gdf5* and *Sox9* was carried out as described (Wilkinson 1992). An acetylation step prior to hybridization was necessary for *Gdf5,* but not for *Sox9.* Plasmid containing *Sox9* (cDNA clone of nt, 116–856; NM_011448) or *Gdf5* (cDNA clone of bp 1321–1871; NM_008109), generously provided by Dr. Eiki Koyama, was transcribed into anti-sense and sense probes using digoxygenin-labeled dNTPs (Fisher). Hybridized samples were incubated with a 1:2000 dilution of alkaline phosphatase-conjugated anti-DIG antibody (Cell Signaling) and developed using an alkaline phosphatase chromogenic substrate (BM Purple, Sigma-Aldrich).

Whole mount *in situ* hybridization using synthesized digoxygenin labeled LNA probe for murine *Acvr1* (Exiqon) followed the recommended Exiqon protocol (Sweetman et al 2006, 2008). Digoxygenin was detected using Vector Blue Alkaline Phosphatase Substrate Kit (SK-5300, Vector Laboratories).

Samples were imaged using an M250C Leica stereomicroscope fitted with a Leica DFC450 C camera.

Results

$Acvr1^{R206H}$ mutation leads to developmental delay in all digits and disrupts digit joint patterning

Our previous studies demonstrated that mice expressing $Acvr1^{R206H}$ recapitulate morphological features of human FOP, including first digit malformations, when expressed globally or in *Prrx1+* limb mesenchymal cells (Chakkalakal et al 2012, 2016). To investigate the effects of the mutation on skeletal development in further detail, the digits of $Acvr1^{R206H/+}$;*Prrx1-Cre* and control embryos (at E14.5) and mice (at P0, P14, and P28) were examined following whole-mount skeletal Alizarin red/Alcian blue staining (Figure 1). At embryonic stage E14.5, cleavage and separation of individual phalanges within the developing digit rays in control mice were complete, resulting in distinct skeletal elements in both forelimbs and hindlimbs. In contrast, cleavage in digits of E14.5 mutant mice at the presumptive digit joints was incomplete in both forelimbs and hindlimbs compared to control littermates (Figure 1A–D). At birth (P0), mineralized bone detected by Alizarin red staining was present in nearly all digit skeletal elements of control mice, but was comparatively reduced in all digits of mutant mice (Figure 1E–H) and was completely absent in mutant hindlimb digit 1 (Figure 1H, H’). Most joints in digits 2, 3, and 4 cleaved over time and showed appropriate separation in mutant hindlimbs, but not forelimbs, with the most notable exception that only two phalanges formed in mutant hindlimb digit 2 instead of the expected three. However, the incomplete joint cleavage phenotype of digits 1 and 5 persisted through early post-natal development.

At P14 (Figure 1I, J, K, L) and P28 (Figure 1 M, N, O, P), we observed dysmorphic digits, absent joints (hindlimb digits 1 and 5; Figure 1K, L, O, P), and absent medial phalanges (hindlimb digits 2 and 5; Figure 1K, L, O, P and forelimb digits 2 through 5; Figure 1I, J, M, N). While joints of control digits showed multiple distinct bands of Alcian blue staining denoting the growth plates and nascent articular cartilage of the interphalangeal joints, a

single band of Alcian blue positive tissue spanned presumptive sites of joint formation in digits of mutant mice with absent joints (Figure 1N, P). Notably, skeletal elements were not equivalently affected within individual digits, a phenotype that persisted over developmental time. At P0, medial and distal phalanges of digits 3 and 4 of mutant mice showed little to no Alizarin red staining compared to the same skeletal elements in control littermates (Figure 1 G, H). Histological analysis was required to assess differences of severity between joints within a single digit (Figure 2; see following section).

Phenotypes were consistent between *Acvr1*$^{R206H/+}$;*Prrx1-Cre* mice and globally-expressed *Acvr1*^{R206H} in *Acvr1*$^{R206H/+}$;*RT;TetO-Cre* knock-in mice (Supplemental Figure 1). These data support that Acvr1^{R206H} delays digit skeletal development and joint formation, with effects most prominent in, but not limited to, digit 1.

Examination of other appendicular skeletal elements in *Acvr1*$^{R206H/+}$;*Prrx1-Cre* mice identified minimal effects on the radius, ulna, and humerus in the forelimb (Supplemental Figure 2B). In contrast, malformations of the femur, fibula, and tibio-fibular joint in the hindlimb (Supplemental Figure 2D) were consistent with previous reports (Chakkalakal et al 2016) showing comparatively short, thick bones. Interestingly, knees and hips of mutants were not fused, supporting site-specific regulation of joint cleavage and development. These data support that *Acvr1*^{R206H} alters skeletal development at multiple sites in addition to the digits, with hindlimb skeletal elements showing greater severity of malformation than forelimb elements.

Growth plates and fused joints in mice expressing Acvr1^{R206H} show aberrant chondrogenesis

The data above suggest a significant disruption of patterning along the proximal-distal axis in digits of mice with FOP. To investigate the specific nature of the altered skeletal morphology, we histologically examined joints and growth plates of *Acvr1*$^{R206H/+}$;*Prrx1-Cre* hindlimb digits in sagittal sections at P14, using Alcian blue to detect cartilage and picrosirius red to detect collagens in bone (Figure 2). Metatarsophalangeal (MTP) joints (between mt and p1 in figure) of controls showed clear separation of skeletal elements, with growth plates arranged orthogonal to the proximal-distal axis. In contrast, digit 1 of mutant mice showed aberrant, expanded areas of chondrogenesis within the skeletal elements, with severely disorganized growth plates aligned along the dorsal-ventral axis rather than the usual proximal-distal polarity (Figure 2B). In addition, most of these (6/7) had incomplete cavitation between skeletal elements (Figure 2A, B). Analysis of digits 2, 3, and 4 revealed more subtle defects (Figure 2C, D; digit 3 is shown). In digit 5 of mutant mice, proximal phalangeal growth plates were broad and disorganized compared to controls, MTP interzones between phalanges were improperly bridged by persisting chondrocytes (7/7), and chondrogenesis was generally expanded within the phalanges (Figure 2E, F).

At P28 (Figure 3), joints of digit 3 and other medial digits in *Acvr1*$^{R206H/+}$;*Prrx1-Cre* mice appeared similar to controls in section histology using picrosirius red and Alcian blue, although all hindlimb digits of mutant mice were significantly reduced in total length at this age (Supplemental Figure 3). The misaligned growth plates that were noted at P14 (Figure 2) remained disorganized and produced cancellous-like bone (Figure 3B, F; asterisks). The

chondrocyte-like joint-bridging cells that were noted at P14 (Figure 2) in mutant digits 1 and 5 persisted in digit 1 (Figure 3B) but were noted in only 4/7 mice in digit 5 (Figure 3F, cleaved example shown). Incomplete cleavage of the MTP joint in digit 1 (6/7) and digit 5 (4/7) in these digits led to a continuous periosteum and thus immobile joints. Interphalangeal joints (between proximal and distal phalanges) of digit 1 and 5 did cleave, however, demonstrating differential effects on different joints within the same digit.

Acvr1^{R206H} leads to dysregulated BMP-pSmad1/5 signaling in embryonic digits

Disruption of the BMP signaling pathway during embryogenesis alters digit patterning, including patterns of chondrogenesis (Brunet et al 1998; reviewed in Pignatti et al 2014). To examine the temporal-spatial activity of the BMP pathway during digit development, we used whole-mount immunohistochemistry of embryonic mouse digits to detect pSMAD1/5 in *Acvr1*$^{R206H/+}$ mutant and control embryos at stages during which pre-patterning of the skeleton occurs (Figure 4).

Reconstructed 3D images revealed a proximal-to-distal alternating pattern of positive and negative staining in control animals, corresponding to regions of bone (pSMAD1/5 positive) and joint (pSMAD1/5 negative) development (notated in Figure 4M). Note that the formation of the hindlimb during embryonic development lagged behind the forelimb by about 12–24 hours, as expected (see control panels in Figure 4A, C, E, G; Shubin and Alberch 1986). Mutant *Acvr1*$^{R206H/+}$;*Prrx1-Cre* littermates showed reduced restriction of pSMAD1/5 staining in the embryonic digits during the earliest stages (E12.0-E12.5) of digit patterning (Figure 4B, D, F, H).

Over developmental time, pSMAD1/5 was progressively restricted to discrete regions within the digit rays in controls. In contrast, mutant limbs lacked the usual restriction of BMP signaling within the digit rays at all time points. By E13.5 in the hindlimbs of mutant mice (Figure 4P), a pattern of proximal-distal BMP pathway activity similar to the control animals at age E12.5 (Figure 4G) began to be apparent, supporting that the *Acvr1*^{R206H} mutation had both delayed the progressive restriction of BMP signaling and disrupted the final pattern of signaling.

To examine whether altered BMP signaling through Acvr1^{R206H} in the mutant digit rays induced downstream effects on chondrogenesis, we performed whole mount *in situ* hybridization to detect expression of *Sox9,* a key regulator of chondrogenesis (Healy et al 1999; Akiyama et al 2002) and direct transcriptional target of BMP pathway signaling and Acvr1^{R206H} (Yoon and Lyons, 2004; Culbert et al., 2014). At E13.5 and E14.5, both control and mutant embryos showed similar diffuse *Sox9* expression patterns in all five digit rays (Supplemental Figure 4A–D). To determine whether effects on chondrogenesis manifested later, we examined histological sections of E16.5 hindlimb digits stained with Alcian Blue. No major differences between control and mutant digits were detected (Supplemental Figure 4E–J). Together, these data indicate that at these early embryonic stages, the effects of the Acvr1^{R206H} mutation on digit joint formation is not indicated by significant changes in chondrogenesis.

The FOP toe malformation and the disruption of BMP-pSmad signaling imply that molecular or genetic interactions through Acvr1 activity differentially contribute to the development and morphology of individual digits. Other BMP type I receptors, such as Bmpr1b, have digit-specific expression patterns or gradients of expression (Hildebrand et al 2019). To examine whether these differences among digits correlate directly to temporal-spatial *Acvr1* expression, we performed whole-mount *in situ* hybridization for *Acvr1* in wild-type embryos (Supplemental Figure 5). *Acvr1* expression was similar in each of the digits. At E12.5, *Acvr1* was expressed in all digit rays and in the interdigit space with no apparent antero-posterior gradient (Supplemental Figure 5A–D). Expression became more restricted to digit periphery at E13.5 (Supplemental Figure 5E–G), and by E14.5 (Supplemental Figure 5H–K), *Acvr1* expression was restricted to digit tips and immediately peripheral to each digit ray with no apparent directional bias in either forelimbs or hindlimbs. These data suggest that interactions of other receptors or ligands, rather than expression bias among digits of *Acvr1* itself, drive the severity of malformation in different digits.

$Acvr1^{R206H}$ alters the distribution of Gdf5-expressing cells in the developing digits

Joint cavitation and the progressive specification of distinct joint tissues depend upon the coordinated migration of *Gdf5*-expressing cells (Koyama et al 2007; Schwartz et al 2016), which can be influenced by the activity of the BMP signaling pathway (Singh et al 2018). While the molecular mechanisms regulating GDF5 activity in the developing joint are still not fully understood, inactivating mutations in *GDF5* in humans are associated with absent phalangeal joints (symphalangism) and the complete absence of the medial phalanges of digits 2 and 5 (Storm and Kingsley 1996; SYM1, MIM#185800). Digits of $Acvr1^{R206H/+}$;*Prrx1-Cre* mice consistently lacked these same skeletal elements (Figure 1L, asterisk). We investigated patterns of *Gdf5* expression in the developing digits of $Acvr1^{R206H/+}$;*Prrx1-Cre* mice by whole mount *in situ* hybridization (ISH). In control mice at E14.5, all presumptive joints were marked by bands of *Gdf5*-expression (Stricker and Mundlos 2011; Figure 5A). In $Acvr1^{R206H/+}$;*Prrx1-Cre* littermates, bands of *Gdf5* expression are discerned in digits 3 and 4, but are absent or diffuse in digits 1 and 2 (Figure 5B). In digit 5, *Gdf5* expression is only visible as a single band, rather than two. However, in all digits of mutant mice, *Gdf5* expression along the periphery of each digit ray is noticeably increased (Figure 5B). To confirm the positions of *Gdf5+* cells, we performed ISH on sectioned autopods at E15.5. As with whole-mount ISH, representative control digits 1, 3, and 5 showed clear transverse bands of *Gdf5*-expressing cells (Supplementary Figure 6A, C, E). *Gdf5* expression in $Acvr1^{R206H/+}$;*Prrx1-Cre* mice appeared qualitatively unchanged in digit 3 (Supplementary Figure 6D), but extended along the perichondrium in digit 5 in addition to expression in the location of the presumptive joint (Supplementary Figure 6F). In digit 1, *Gdf5* expression was detected only peripherally (Supplementary Figure 6B), demonstrating a severe disruption of the localization of *Gdf5+* presumptive joint progenitor cells in this digit. These data suggest that *Gdf5* expression patterns are in part determined by Acvr1 signaling activity and that digit 1 is acutely sensitive to the effects of dysregulated Acvr1 signaling.

Discussion

We have determined that the expression of the Acvr1-R206H mutant receptor in *Prrx1*$^{+}$ cells confers a joint formation defect that impacts all embryonic digit rays, resulting in developmental delay with impaired interzone formation and joint cavitation. Enhanced signaling by this activating mutation, which has been shown to be both ligand-independent and ligand-responsive (Shen et al 2009; Allen et al 2020), yields fused, malformed joints and digit skeletal elements (phalanges) with disrupted endochondral ossification at growth plates that impacts all digits. These effects are most pronounced in the hindlimb first digit (great toe), with digit 5 also significantly altered, while digits 2, 3, and 4 are impacted to lesser extents. Our current study has focused on digit development; however, we note that the Acvr1-R206H mutation also perturbs development and joint formation at multiple sites throughout the appendicular skeleton, with hindlimbs more affected than forelimbs.

Disrupted proximal-distal patterning of the digit rays in Acvr1$^{R206H/+}$ mice

The importance of the BMP pathway in digit and joint development is well established (Brunet et al 1998; Gamer et al 2011, reviewed in Lyons and Rosen 2019); however, due to its multiple biological roles and interacting pathways, elucidating detailed mechanisms and functions of BMP signaling in skeletal development and function continues to be of great scientific and clinical interest. Regions of high BMP pathway activity initiate the chondrogenic program to pre-pattern the cartilaginous skeleton by (Foster et al 1994). Conversely, BMP pathway activity must be restricted during skeletal patterning to permit the differentiation and development of joint tissues (Bandyopadhyay et al 2006). Using whole-mount immunohistochemistry with confocal microscopy to capture the full detail of canonical BMP pathway activity during limb embryogenesis, we determined that in *Acvr1*$^{R206H/+}$;*Prrx1-Cre* mice, BMP pathway activity is not appropriately restricted at sites of presumptive joint formation within the digit rays between E12.0 and E13.5, a period of rapid growth and pre-patterning of the cartilage skeleton template. The expanded regions of signaling parallel the aberrantly unsegmented cartilaginous skeleton of the digits just 24 hours later at E14.5 (compare Figure 1B, D and Figure 4H, P) demonstrating a direct effect of dysregulated Acvr1-pSmad1/5 signaling.

Joint development and interzone formation occur in a proximal-to-distal pattern as the skeleton forms over developmental time during embryogenesis. In genetic and bead-implant models of enhanced or dysregulated BMP pathway signaling, failed joint cleavage and separation of the affected developing skeletal elements are associated with reduced appearance and/or migration of *Gdf5+* cells in the nascent joint interzone, preventing cleavage and altering the total number of phalanges in the final structure of the digit ray (Brunet et al 1998; Dahn and Fallon 2000; Huang et al 2018; Singh et al 2018). In our *Acvr1*^{R206H} model, *Gdf5* expression in the presumptive interzone of specific digits is drastically reduced and phalanx numbers in digits 2 and 5 are reduced. These data support a model in which increased BMP pathway signaling through any means, whether gain-of-function mutations of receptors and ligands (Klammer et al 2015; Singh et al 2018) or loss-of-function of inhibitors (Brunet et al 1998), impairs digit joint patterning despite the discrete roles of those molecules in development (Zou et al 1997). Thus, not only does the

Acvr1-R206H mutation cause delayed restriction of pSmad1/5, but also subsequently disrupts the overall process of joint formation in specific joints.

Specific malformation of individual digits through Acvr1 R206H

In *Acvr1*$^{R206H/+}$;*Prrx1-Cre* mice, dysregulated BMP pathway signaling is most evident in the first digit of the mutant hindlimb, consistent with the highly penetrant phenotype of shortened and/or malformed first digits of the feet of human patients with FOP. We have determined that while digit 1 is the most severely affected, other digits and joints of the developing skeleton are also altered. *Acvr1* expression domains appear similar in all digit rays, supporting that a digit-specific bias of where *Acvr1* is expressed at the stages we examined (E12.5-E14.5) does not correlate with the differences in digit malformations induced by the Acvr1 mutation. Indeed, while all digit rays show altered pSmad1/5 localization during embryogenesis, digits 1 and 5 are more dysmorphic at post-natal stages than digits 2, 3, and 4. Therefore, the variability of the phenotype among digits is not solely dependent on Acvr1 but likely is due to altered interactions between Acvr1-R206H and other components of the BMP signaling pathway, or perhaps other interacting pathways. Within a single digit, joints form through an iterative process from proximal to distal over developmental time (Suzuki et al 2008). Therefore, the different effects of Acvr1 mutation on different joints within a single digit – for example, in *Acvr1*^{R206H}, the fused metatarsophalangeal joint of digit 1 and the fully cleaved distal interphalangeal joint (Figure 3B) – suggests that the iterative pattern of phalanx and phalanx joint formation in digits may be differently affected over developmental time, perhaps by modulating the Turing mechanism that has been proposed for regulating digit and digit joint specification (Raspopovic et al 2014; Scoones and Hiscock 2020).

Gdf5 is a member of the BMP ligand superfamily that is critical for joint development. Deletion of Gdf5 leads to total joint fusion with the most severe phenotypes in the most distal skeletal elements, i.e., the digits (Storm et al 1994). Unlike the signaling activity of other BMP ligands, such as BMP2, which must be decreased in the joint interzone, *Gdf5* expression is required to specify joint formation (Koyama et al 2008). In normal development, *Gdf5* expression is observed in nascent skeletal elements, but rapidly resolves into bands of expression at the positions of future joints of digits and other long bones, with digits 1 and 5 lagging behind digits 2 through 4 (Stricker and Mundlos 2011). *Gdf5*-expressing mesenchymal cells first organize in the periphery of the presumptive joints before migrating into the joint interzone (Koyama et al 2008; reviewed in Decker 2016) and differentiating into specific joint tissues (Schwartz et al 2016). We determined that *Gdf5* expression patterns are perturbed in *Acvr1*$^{R206H/+}$;*Prrx1-Cre* mice, particularly in digits 1 and 5, with *Gdf5*-expressing cells localized in a comparatively expanded region of the periphery of digits 1 and 5, rather than across the developing joint space. Downstream of these developmental events, hindlimb joints of *Acvr1*^{R206H} mice, particularly in digits 1 and 5, are severely malformed, fail to fully cleave to form joints, and are not fully functional. These results are consistent with findings showing the critical importance of both the timing of the influx of *Gdf5*-expressing cells (Schwartz et al 2016) and the spatial restriction of BMP pathway activity (Ray et al 2015) for the appropriate differentiation of joint progenitor cells and their contributions to the specific tissues that constitute a properly patterned joint.

Further, lineage tracing experiments have shown that cells in the most anterior and most posterior regions of the autopod (hand and foot) including all of digit 1, the anterior portion of digit 2, and much of digit 5, descend from *Gdf5*-expressing cells, whereas these cells are only found in close proximity to digit joints in digits 3 and 4 (Rountree et al 2004). Although the digit and joint specificity of Acvr1^{R206H} effects requires further detailed examination, we note that this mutant receptor has altered ligand responsiveness (Hatsell et al 2015, Allen et al 2020). ACVR1-R206H has been shown to have acquired increased responsiveness to known (BMPs) and atypical (Activin A) ligands, as well as possessing ligand-independent signaling activity, suggesting the possibility that the available ligand repertoire could also influence responses at specific joints and supporting a model in which altered interaction between mutant Acvr1 and Gdf5 ligands allows the mutant receptor to specifically affect some digits more than others.

An alternative mechanism by which *Acvr1* mutation may exhibit different effects on specific digits is through variable BMP signaling complex formation during early development and patterning due to patterns of expression. During development, *Acvr1* is expressed with no apparent gradient or bias (Supplemental Figure 5). In contrast, *Bmpr1a (Alk3)* expression during early development shows increased posterior expression compared to anterior (Rountree et al 2004) and *Bmpr1b (Alk6)* is strongly expressed in digits 2–5, but weakly expressed in digit 1 (Hildebrandt et al 2019). Thus, digit 1 may be particularly susceptible to Acvr1 mutation and/or loss of the other type I receptors. Indeed, our data show that the activating FOP *Acvr1^{R206H}* mutation in mice leads to a phenotype similar to *Bmpr1b* knock-out (Baur et al 2000). Additionally, deletion of an extensive region of *BMPR1B* caused a FOP-like digit phenotype (Towler et al 2017). Not just type I receptors, but also relative levels of ligand may be similarly responsible. For instance, combinatorial knockouts of Bmp2, Bmp4, and Bmp7 yield digit-specific ablations or duplications (Bandyopadhyay et al 2006). Therefore, digit specificity of the FOP phenotype may be influenced through a relative abundance of other type I receptors or responsiveness to specific ligands; however, further experiments are needed to confirm such a hypothesis.

Aberrant endochondral ossification due to Acvr1-R206H

In normal development, chondrocytes in long bones differentiate to form either articular cartilage at the ends of bones, which persists throughout life, or growth plate cartilage, which contributes to the longitudinal growth of the bone via organized, stratified cell growth, proliferation, and endochondral ossification (reviewed in Lefebvre and Smits 2005). Previous work reported growth plate defects in tibias of P7 and P14 Acvr1^{R206H} mice (Chakkalakal et al 2012, 2016). In the current study, a developmental time course identified that impaired joint formation during embryonic development is followed by severely altered growth plate polarity, delayed turnover of cartilage to bone in the digits, and ectopic, disorganized chondrogenesis along interior, medial surfaces of phalanges. In murine digits 1 and 5, joints failed to fully cleave during embryonic skeletal development. In the presumptive joints of these digits, a persistent chondrocytic bridge joined normally separate skeletal elements (phalanges), and distinct secondary ossification centers or epiphyses did not form. These regions of disordered chondrocytes resulted in a significant impact on the final morphology of the bones. These data suggest that Acvr1^{R206H} not only directs aberrant

ectopic chondrogenesis and endochondral ossification in soft connective tissues (heterotopic ossification) as observed in FOP patients and mouse models, but also leads to disrupted endochondral ossification in the endogenous skeleton.

Based on *in vitro* data showing elevated levels of *Sox9* expression in response to BMP ligand in $Acvr1^{R206H/+}$ cells (Culbert et al., 2014) and increased Sox9 detected in $Acvr1^{R206H}$ growth plates *in vivo* at P14 (Chakkalakal et al., 2016), we expected that altered *Sox9* expression would be detected in the developing $Acvr1^{R206H}$ skeleton. At the early embryonic stages examined (E13.5-E14.5), we found no differences in the localization of *Sox9* expression, and at E16.5, chondrogenic maturation in the mutants and control was similar suggesting that elevated BMP signaling and levels of *Sox9* were not driving an increased rate of chondrogenic differentiation during these developmental stages. However, delayed progression to endochondral ossification is evident by birth (P0; Figure 1), indicating that chondrogenesis has been impacted prior to this time. A more detailed examination of later stages of embryonic development will be necessary to determine the molecular mediators and pathways downstream of $Acvr1^{R206H}$ signaling. We also note that the $Acvr1^{R206H}$ mutation is not a strongly constitutively activating mutation (Shen et al 2009, Culbert et al 2014), and therefore suggest that low level activation of Acvr1 signaling and *Sox9* expression is insufficient to significantly impact chondrogenesis during early embryonic development, but over developmental time begins to alter the chondrogenic and endochondral phenotype. Previous studies reported that tibial growth plates of $Acvr1^{R206H}$ mice at P14 have longer epiphyseal zones and shorter hypertrophic zones (Chakkalakal et al 2016), suggesting an expansion of proliferative and/or pre-hypertrophic chondrocytes, but restricted rates of hypertrophy and maturation in response to $Acvr1^{R206H}$.

Of note, our findings in the $Acvr1^{R206H}$ digits are highly similar to limb-specific knock-out of *Indian hedgehog (Ihh)*, in which $Gdf5^{+}$ progenitor cells are found flanking the joint interzone, but not within the interzone itself (Koyama et al 2007; Amano et al 2016). Further, the adult phenotype of our model closely matches the *brachypodism Gdf5* loss-of-function mouse line, including specific disruption of digits 1, 2, and 5 as well as dysmorphic sesamoids (Storm et al 1994). Because our data show altered localization of *Gdf5* expression, this may indicate either a direct interaction between Acvr1-R206H and Gdf5 as suggested above or an indirect interaction through Ihh. We postulate a direct effect is more likely because Gdf5 is a BMP ligand.

Our data clearly demonstrate the impact of $Acvr1^{R206H}$ on processes of digit joint and skeletal development. The mutation dysregulates BMP pathway activity within the digit ray, which results in altered distribution of *Gdf5+* cells and thus joint cavitation. Detailed examination of embryonic developmental stages is required to address the precise sequence of events and pathways through which Acvr1 signaling regulates *Gdf5* and joint formation. Future studies investigating interactions among Ihh activity, Gdf5 ligand, and BMP pathway signaling through Acvr1 will begin to elucidate this mechanism.

Clinical relevance of skeletal and joint malformation in FOP

Skeletal malformations at multiple anatomic sites have been occasionally noted in FOP patients with the ACVR1 R206H mutation (Kaplan et al 2009). The data reported here,

together with prior work with this mouse model (Chakkalakal et al 2016), show that Acvr1-R206H alters chondrogenic differentiation during skeletal development, particularly at sites of joint formation, which leads to malformed adult structures with reduced function. This altered chondrogenesis appears likely to be the cellular basis of skeletal dysmorphia in the FOP population such as in the metatarsal and phalanges of the great toe (Tünte et al 1967; Nakashima et al 2010) and femoral neck (Kaplan et al 2009), as well as tibial and femoral osteochondromas, which are common features of FOP (Kaplan et al 2009; Morales-Piga et al 2015). Further, Acvr1-R206H alters patterns of *Gdf5* expression, and *GDF5* mutations have been associated with joint deformity and dysplasia (Storm et al 1994; Hatzikotoulas et al 2018). These data led to a complementary study of the skeleton in a large cohort of FOP patients, which identified joint malformations, dysplasia, severe degenerative arthropathy, and intra-articular ankylosis in a high percentage of patients at stereotypical sites (Towler et al 2019). Together, these and future studies will provide a clearer understanding of the role of ACVR1 in joint development, disease, and degeneration, as well as the developmental impact of the ACVR1-R206H mutation on skeletal maintenance and function, which will support further steps to improve the quality of life for those with FOP.

Conclusions

These studies provide insight into the molecular regulation of site-specific joint and skeletal development through ACVR1 and BMP pathway signaling through the lens of a disease-causing, activating mutation in ACVR1. Dysregulation of the Acvr1-BMP pathway impairs skeletal patterning by altering the distribution of *Gdf5*-expressing joint progenitor cells and by delaying and disrupting joint cleavage and endochondral ossification during joint formation. These effects are downstream of increased BMP signaling during early embryonic limb development that disrupts the usual patterning of BMP pathway activity. Our data reinforce the importance of BMP pathway restriction during this critical developmental process and the contributions of this pathway through the ACVR1 receptor to skeletal and joint morphology.

Supplementary Material

Refer to Web version on PubMed Central for supplementary material.

Acknowledgments

We thank Deyu Zheng, Bob Caron, and Dr. Salin Chakkalakal for their input and technical assistance with histology and mouse breeding, and the other members of our lab for valuable comments and discussion. We thank Dr. Maurizio Pacifici for insights and advice regarding skeletal development. We are deeply grateful to Drs. Joseph Zinski and Andrea Stout for training, expertise, and methods development with confocal microscopy. Thank you to Dr. Eiki Koyama for the gift of the *Gdf5* and *Sox9 in situ* RNA probe. Thank you to Dr. Terence Cappelini and his lab for *in situ* hybridization protocol advice for *Gdf5*. We thank Regeneron Pharmaceuticals for developing the knock-in mouse model of FOP ($Acvr1^{[R206H]FlEx}$) used in these studies.

This work was supported by a grant from the International Fibrodysplasia Ossificans Progressiva Association (IFOPA), the Center for Research in FOP and Related Disorders, the Ian Cali Endowment for FOP Research, the Whitney Weldon Endowment for FOP Research, the Cali-Weldon Professorship of FOP Research (EMS), the Isaac and Rose Nassau Professorship of Orthopaedic Molecular Medicine (FSK), and the National Institutes of Health (F32AR071298 to SHP). Histology and imaging core facility resources were through the Penn Center for Musculoskeletal Disorders (NIH P30-AR050950).

References

Ahn K; Mishina Y; Hanks MC; Behringer RR; Crenshaw EB BMPR-IA Signaling Is Required for the Formation of the Apical Ectodermal Ridge and Dorsal-Ventral Patterning of the Limb. Development 2001, 128 (22), 4449–4461. [PubMed: 11714671]

Akiyama H; Chaboissier M-C; Martin JF; Schedl A; Crombrugghe B. de. The Transcription Factor Sox9 Has Essential Roles in Successive Steps of the Chondrocyte Differentiation Pathway and Is Required for Expression of Sox5 and Sox6. Genes Dev. 2002, 16 (21), 2813–2828. 10.1101/gad.1017802. [PubMed: 12414734]

Allen RS, Tajer B, Shore EM, Mullins MC. Fibrodysplasia ossificans progressiva mutant ACVR1 signals by multiple modalities in the developing zebrafish. eLife. 9. doi:10.7554/eLife.53761.

Amano K; Densmore M; Fan Y; Lanske B. Ihh and PTH1R Signaling in Limb Mesenchyme Is Required for Proper Segmentation and Subsequent Formation and Growth of Digit Bones. Bone 2016, 83, 256–266. 10.1016/j.bone.2015.11.017. [PubMed: 26620087]

Bandyopadhyay A; Tsuji K; Cox K; Harfe BD; Rosen V; Tabin CJ Genetic Analysis of the Roles of BMP2, BMP4, and BMP7 in Limb Patterning and Skeletogenesis. PLoS Genet 2006, 2 (12). 10.1371/journal.pgen.0020216.

Brunet LJ; McMahon JA; McMahon AP; Harland RM Noggin, Cartilage Morphogenesis, and Joint Formation in the Mammalian Skeleton. Science 1998, 280 (5368), 1455–1457. 10.1126/science.280.5368.1455. [PubMed: 9603738]

Chakkalakal SA; Zhang D; Culbert AL; Convente MR; Caron RJ; Wright AC; Maidment AD; Kaplan FS; Shore EM An *Acvr1* R206H Knock-in Mouse Has Fibrodysplasia Ossificans Progressiva. J. Bone Miner. Res. 2012, 27 (8), 1746–1756. 10.1002/jbmr.1637. [PubMed: 22508565]

Chakkalakal SA; Uchibe K; Convente MR; Zhang D; Economides AN; Kaplan FS; Pacifici M; Iwamoto M; Shore EM Palovarotene Inhibits Heterotopic Ossification and Maintains Limb Mobility and Growth in Mice With the Human ACVR1(R206H) Fibrodysplasia Ossificans Progressiva (FOP) Mutation. J. Bone Miner. Res. 2016, 31 (9), 1666–1675. 10.1002/jbmr.2820. [PubMed: 26896819]

Chen H; Capellini TD; Schoor M; Mortlock DP; Reddi AH; Kingsley DM Heads, Shoulders, Elbows, Knees, and Toes: Modular Gdf5 Enhancers Control Different Joints in the Vertebrate Skeleton. PLOS Genetics 2016, 12 (11), e1006454. 10.1371/journal.pgen.1006454.

Culbert AL, Chakkalakal SA, Theosmy EG, Brennan TA, Kaplan FS, Shore EM. Alk2 regulates early chondrogenic fate in fibrodysplasia ossificans progressiva heterotopic endochondral ossification. Stem Cells. 2014;32(5):1289–1300. doi:10.1002/stem.1633. [PubMed: 24449086]

Dahn RD; Fallon JF Interdigital Regulation of Digit Identity and Homeotic Transformation by Modulated BMP Signaling. Science 2000, 289 (5478), 438–441. 10.1126/science.289.5478.438. [PubMed: 10903202]

Decker RS Articular Cartilage and Joint Development from Embryogenesis to Adulthood. Seminars in Cell & Developmental Biology 2017, 62, 50–56. 10.1016/j.semcdb.2016.10.005. [PubMed: 27771363]

Foster JW; Dominguez-Steglich MA; Guioli S; Kwok C; Weller PA; Stevanović M; Weissenbach J; Mansour S; Young ID; Goodfellow PN Campomelic Dysplasia and Autosomal Sex Reversal Caused by Mutations in an SRY-Related Gene. Nature 1994, 372 (6506), 525–530. 10.1038/372525a0. [PubMed: 7990924]

Gamer LW; Tsuji K; Cox K; Capelo LP; Lowery J; Beppu H; Rosen V. BMPR-II Is Dispensable for Formation of the Limb Skeleton. Genesis 2011, 49 (9), 719–724. 10.1002/dvg.20761. [PubMed: 21538804]

Harrison RJ; Pitcher JD; Mizel MS; Temple HT; Scully SP The Radiographic Morphology of Foot Deformities in Patients with Fibrodysplasia Ossificans Progressiva. Foot Ankle Int 2005, 26 (11), 937–941. 10.1177/107110070502601107. [PubMed: 16309607]

Hatsell SJ; Idone V; Wolken DMA; Huang L; Kim HJ; Wang L; Wen X; Nannuru KC; Jimenez J; Xie L; et al. ACVR1 R206H Receptor Mutation Causes Fibrodysplasia Ossificans Progressiva by Imparting Responsiveness to Activin A. Sci. Trans. Med. 2015, 7 (303), 303ra137–303ra137. 10.1126/scitranslmed.aac4358.

Hatzikotoulas K; Roposch A; Shah KM; Clark MJ; Bratherton S; Limbani V; Steinberg J; Zengini E; Warsame K; Ratnayake M; et al. Genome-Wide Association Study of Developmental Dysplasia of the Hip Identifies an Association with GDF5. Comms. Bio. 2018, 1 (1). 10.1038/s42003-018-0052-4.

Healy C; Uwanogho D; Sharpe PT Regulation and Role of Sox9 in Cartilage Formation. Dev. Dyn. 1999, 215 (1), 69–78. 10.1002/(SICI)10970177(199905)215:1<69::AID-DVDY8>3.0.CO;2-N. [PubMed: 10340758]

Hildebrand L; Kegler MS; Walther M; Seemann P; Stange K. Limb Specific Acvr1-Knockout during Embryogenesis in Mice Exhibits Great Toe Malformation as Seen in Fibrodysplasia Ossificans Progressiva (FOP). Dev. Dyn. 2019. 10.1002/dvdy.24.

Huang B-L; Trofka A; Furusawa A; Norrie JL; Rabinowitz AH; Vokes SA; Mark Taketo M; Zakany J; Mackem S. An Interdigit Signalling Centre Instructs Coordinate Phalanx-Joint Formation Governed by 5′Hoxd–Gli3 Antagonism. Nat. Commun. 2016, 7. 10.1038/ncomms12903.

Jean McLeod M. Differential Staining of Cartilage and Bone in Whole Mouse Fetuses by Alcian Blue and Alizarin Red S. Teratology 1980, 22, 299–301. 10.1002/tera.1420220306. [PubMed: 6165088]

Kaplan FS; Xu M; Glaser DL; Collins F; Connor M; Kitterman J; Sillence D; Zackai E; Ravitsky V; Zasloff M; et al. Early Diagnosis of Fibrodysplasia Ossificans Progressiva. Pediatrics 2008, 121 (5), e1295–e1300. 10.1542/peds.2007-1980.

Kaplan FS; Xu M; Seemann P; Connor JM; Glaser DL; Carroll L; Delai P; Fastnacht-Urban E; Forman SJ; Gillessen-Kaesbach G; et al. Classic and Atypical Fibrodysplasia Ossificans Progressiva (FOP) Phenotypes Are Caused by Mutations in the Bone Morphogenetic Protein (BMP) Type I Receptor ACVR1. Hum. Mutat. 2009, 30 (3), 379–390. 10.1002/humu.20868. [PubMed: 19085907]

Klammert U; Mueller TD; Hellmann TV; Wuerzler KK; Kotzsch A; Schliermann A; Schmitz W; Kuebler AC; Sebald W; Nickel J. GDF-5 Can Act as a Context-Dependent BMP-2 Antagonist. BMC Biology 2015, 13 (1). 10.1186/s12915-015-0183-8.

Koyama E; Ochiai T; Rountree RB; Kingsley DM; Enomoto-Iwamoto M; Iwamoto M; Pacifici M. Synovial Joint Formation during Mouse Limb Skeletogenesis: Roles of Indian Hedgehog Signaling. Ann. NY Acad. Sci. 2007, 1116 (1), 100–112. 10.1196/annals.1402.063. [PubMed: 18083924]

Koyama E; Shibukawa Y; Nagayama M; Sugito H; Young B; Yuasa T; Okabe T; Ochiai T; Kamiya N; Rountree RB; et al. A Distinct Cohort of Progenitor Cells Participates in Synovial Joint and Articular Cartilage Formation during Mouse Limb Skeletogenesis. Dev. Biol. 2008, 316 (1), 62–73. 10.1016/j.ydbio.2008.01.012. [PubMed: 18295755]

Lefebvre V; Smits P. Transcriptional Control of Chondrocyte Fate and Differentiation. BDRC 2005, 75 (3), 200–212. 10.1002/bdrc.20048.

Logan M, Martin JF, Nagy A, Lobe C, Olson EN, Tabin CJ. Expression of Cre Recombinase in the developing mouse limb bud driven by a Prxl enhancer. Genesis. 2002;33(2):77–80. doi:10.1002/gene.10092. [PubMed: 12112875]

Lyons KM; Rosen V. BMPs, TGFβ, and Border Security at the Interzone. In Curr. Top. Dev. Biol.; Elsevier, 2019; Vol. 133, pp 153–170. 10.1016/bs.ctdb.2019.02.001. [PubMed: 30902251]

McGlinn E; Mansfield JH Detection of Gene Expression in Mouse Embryos and Tissue Sections. In Vertebrate Embryogenesis: Embryological, Cellular, and Genetic Methods; Pelegri FJ, Ed.; Methods in Molecular Biology; Humana Press: Totowa, NJ, 2011; pp 259–292. 10.1007/978-1-61779-210-6_10.

Merino R; Rodriguez-Leon J; Macias D; Ganan Y; Economides AN; Hurle JM The BMP Antagonist Gremlin Regulates Outgrowth, Chondrogenesis and Programmed Cell Death in the Developing Limb. Development 1999, 126 (23), 5515–5522. [PubMed: 10556075]

Mitrovic DR Development of the Metatarsophalangeal Joint of the Chick Embryo: Morphological, Ultrastructural and Histochemical Studies. Am. J. Anat. 1977, 150 (2), 333–347. 10.1002/aja.1001500207. [PubMed: 920633]

Morales-Piga A; Bachiller-Corral J; González-Herranz P; Medrano-SanIldelfonso M; Olmedo-Garzón J; Sánchez-Duffhues G. Osteochondromas in Fibrodysplasia Ossificans Progressiva: A Widespread Trait with a Streaking but Overlooked Appearance When Arising at Femoral Bone End. Rheumatol. Int. 2015, 35 (10), 1759–1767. 10.1007/s00296-015-3301-6. [PubMed: 26049728]

Nakashima Y; Haga N; Kitoh H; Kamizono J; Tozawa K; Katagiri T; Susami T; Fukushi J; Iwamoto Y. Deformity of the Great Toe in Fibrodysplasia Ossificans Progressiva. J. Orthop. Sci. 2010, 15 (6), 804–809. 10.1007/s00776-010-1542-5. [PubMed: 21116899]

Norrie JL; Lewandowski JP; Bouldin CM; Amarnath S; Li Q; Vokes MS; Ehrlich LIR; Harfe BD; Vokes SA Dynamics of BMP Signaling in Limb Bud Mesenchyme and Polydactyly. Dev Bio 2014, 393 (2), 270–281. 10.1016/j.ydbio.2014.07.003. [PubMed: 25034710]

Pignatti E; Zeller R; Zuniga A. To BMP or Not to BMP during Vertebrate Limb Bud Development. Seminars in Cell & Developmental Biology 2014, 32, 119–127. 10.1016/j.semcdb.2014.04.004. [PubMed: 24718318]

Pizette S; Niswander L. BMPs Are Required at Two Steps of Limb Chondrogenesis: Formation of Prechondrogenic Condensations and Their Differentiation into Chondrocytes. Dev Bio 2000, 219 (2), 237–249. 10.1006/dbio.2000.9610. [PubMed: 10694419]

Raspopovic J, Marcon L, Russo L, Sharpe J. Digit patterning is controlled by a Bmp-Sox9-Wnt Turing network modulated by morphogen gradients. Science. 2014;345(6196):566–570. doi:10.1126/science.1252960. [PubMed: 25082703]

Ray A; Singh PNP; Sohaskey ML; Harland RM; Bandyopadhyay A. Precise Spatial Restriction of BMP Signaling Is Essential for Articular Cartilage Differentiation. Development 2015, 142 (6), 1169–1179. 10.1242/dev.110940. [PubMed: 25758226]

Richardson L; Venkataraman S; Stevenson P; Yang Y; Moss J; Graham L; Burton N; Hill B; Rao J; Baldock RA; et al. EMAGE Mouse Embryo Spatial Gene Expression Database: 2014 Update. Nucleic Acids Res. 2014, 42 (D1), D835–D844. 10.1093/nar/gkt1155. [PubMed: 24265223]

Rigueur D; Brugger S; Anbarchian T; Kim JK; Lee Y; Lyons KM The Type I BMP Receptor ACVR1/ALK2 Is Required for Chondrogenesis During Development: Role of ALK2 in Chondrogenesis. J. Bone Miner. Res. 2015, 30 (4), 733–741. 10.1002/jbmr.2385. [PubMed: 25413979]

Rountree RB; Schoor M; Chen H; Marks ME; Harley V; Mishina Y; Kingsley DM BMP Receptor Signaling Is Required for Postnatal Maintenance of Articular Cartilage. PLoS Biology 2004, 2 (11), e355. 10.1371/journal.pbio.0020355.

Schindelin J; Arganda-Carreras I; Frise E; Kaynig V; Longair M; Pietzsch T; Preibisch S; Rueden C; Saalfeld S; Schmid B; et al. Fiji: An Open-Source Platform for Biological-Image Analysis. Nat. Methods 2012, 9 (7), 676–682. 10.1038/nmeth.2019. [PubMed: 22743772]

Schroeder HW; Zasloff M. The Hand and Foot Malformations in Fibrodysplasia Ossificans Progressiva. Johns Hopkins Med. J. 1980, 147 (2), 73–78. [PubMed: 7412069]

Scoones JC, Hiscock TW. A dot-stripe Turing model of joint patterning in the tetrapod limb. Development. 2020;147(8):dev183699. doi:10.1242/dev.183699.

Settle SH; Rountree RB; Sinha A; Thacker A; Higgins K; Kingsley DM Multiple Joint and Skeletal Patterning Defects Caused by Single and Double Mutations in the Mouse Gdf6 and Gdf5 Genes. Dev. Biol. 2003, 254 (1), 116–130. 10.1016/S0012-1606(02)00022-2. [PubMed: 12606286]

Shen Q; Little SC; Xu M; Haupt J; Ast C; Katagiri T; Mundlos S; Seemann P; Kaplan FS; Mullins MC; et al. The Fibrodysplasia Ossificans Progressiva R206H ACVR1 Mutation Activates BMP-Independent Chondrogenesis and Zebrafish Embryo Ventralization. J. Clin. Invest. 2009, 119 (11), 3462–3472. 10.1172/JCI37412. [PubMed: 19855136]

Shore EM; Xu M; Feldman GJ; Fenstermacher DA; Cho T-J; Choi IH; Connor JM; Delai P; Glaser DL; LeMerrer M; et al. A Recurrent Mutation in the BMP Type I Receptor ACVR1 Causes Inherited and Sporadic Fibrodysplasia Ossificans Progressiva. Nat. Gen. 2006, 38 (5), 525–527. 10.1038/ng1783.

Shubin NH; Alberch P. A Morphogenetic Approach to the Origin and Basic Organization of the Tetrapod Limb. In Evolutionary Biology: Volume 20; Hecht MK, Wallace B, Prance GT, Eds.; Springer US: Boston, MA, 1986; pp 319–387. 10.1007/978-1-4615-6983-1_6.

Shwartz Y; Viukov S; Krief S; Zelzer E. Joint Development Involves a Continuous Influx of Gdf5-Positive Cells. Cell Reports 2016, 15 (12), 2577–2587. 10.1016/j.celrep.2016.05.055. [PubMed: 27292641]

Singh PNP; Shea CA; Sonker SK; Rolfe RA; Ray A; Kumar S; Gupta P; Murphy P; Bandyopadhyay A. Precise Spatial Restriction of BMP Signaling in Developing Joints Is Perturbed upon Loss of Embryo Movement. Development 2018, 145 (5), dev153460. 10.1242/dev.153460.

Storm EE; Kingsley DM Joint Patterning Defects Caused by Single and Double Mutations in Members of the Bone Morphogenetic Protein (BMP) Family. 1996, No. 122, 3969–3979.

Storm EE; Huynh TV; Copeland NG; Jenkins NA; Kingsley DM; Lee S-J Limb Alterations in Brachypodism Mice Due to Mutations in a New Member of the TGFβ-Superfamily. Nature 1994, 368 (6472), 639–643. 10.1038/368639a0. [PubMed: 8145850]

Stricker S; Mundlos S. Mechanisms of Digit Formation: Human Malformation Syndromes Tell the Story. Dev Bio 2011, 240 (5), 990–1004. 10.1002/dvdy.22565.

Suzuki T, Hasso SM, Fallon JF. Unique SMAD1/5/8 activity at the phalanx-forming region determines digit identity. Proc Natl Acad Sci USA. 2008;105(11):4185–4190. doi:10.1073/pnas.0707899105. [PubMed: 18334652]

Sweetman D; Rathjen T; Jefferson M; Wheeler G; Smith TG; Wheeler GN; Münsterberg A; Dalmay T. FGF-4 Signaling Is Involved in Mir-206 Expression in Developing Somites of Chicken Embryos. Dev. Dyn. 2006, 235 (8), 2185–2191. 10.1002/dvdy.20881. [PubMed: 16804893]

Sweetman D; Goljanek K; Rathjen T; Oustanina S; Braun T; Dalmay T; Münsterberg A. Specific Requirements of MRFs for the Expression of Muscle Specific MicroRNAs, MiR-1, MiR-206 and MiR-133. Dev. Biol. 2008, 321 (2), 491–499. 10.1016/j.ydbio.2008.06.019. [PubMed: 18619954]

Towler OW; Shore EM; Xu M; Bamford A; Anderson I; Pignolo RJ; Kaplan FS The Congenital Great Toe Malformation of Fibrodysplasia Ossificans Progressiva? - A Close Call. Eur J Med Genet 2017, 60 (7), 399–402. 10.1016/j.ejmg.2017.04.013. [PubMed: 28473268]

Towler OW, Shore EM, Kaplan FS. Skeletal malformations and developmental arthropathy in individuals who have fibrodysplasia ossificans progressiva. Bone. Published online October 23, 2019:115116. doi:10.1016/j.bone.2019.115116.

Tünte W; Becker PE; Knorre G.v. Zur Genetik der Myositis ossificans progressiva. Hum Genet 1967, 4 (4), 320–351. 10.1007/BF00285740.

Wilkinson DG Whole Mount in Situ Hybridization of Vertebrate Embryos. In Situ Hybridization: A Practical Approach. Edited by: Wilkinson DG. 1992; Oxford University Press, Oxford.

Wu M; Chen G; Li Y-P TGF-β and BMP Signaling in Osteoblast, Skeletal Development, and Bone Formation, Homeostasis and Disease. Bone Res 2016, 4, 16009. 10.1038/boneres.2016.9. [PubMed: 27563484]

Yokomizo T; Yamada-Inagawa T; Yzaguirre AD; Chen MJ; Speck NA; Dzierzak E. Whole-Mount Three-Dimensional Imaging of Internally Localized Immunostained Cells within Mouse Embryos. Nature Protocols 2012, 7 (3), 421–431. 10.1038/nprot.2011.441. [PubMed: 22322215]

Yoon BS; Lyons KM Multiple Functions of Bmps in Chondrogenesis. J Cell Biochem. 2004, 93–103. [PubMed: 15352166]

Zou H; Wieser R; Massagué J; Niswander L. Distinct Roles of Type I Bone Morphogenetic Protein Receptors in the Formation and Differentiation of Cartilage. Genes Dev 1997, 11 (17), 2191–2203. [PubMed: 9303535]

Highlights

- The BMP type I receptor Acvr1 is a key regulator of digit and joint formation in early development.
- Dysregulated BMP signaling caused by the R206H mutation in Acvr1, a common mutation in the human genetic disorder FOP, inhibits joint development in multiple murine digits and induces aberrant endochondral ossification at developing growth plates.
- Acvr1-R206H dysregulates temporal-spatial restriction of BMP pathway signaling, joint interzone formation, and localization of *Gdf5*-expressing cells during skeletal development.

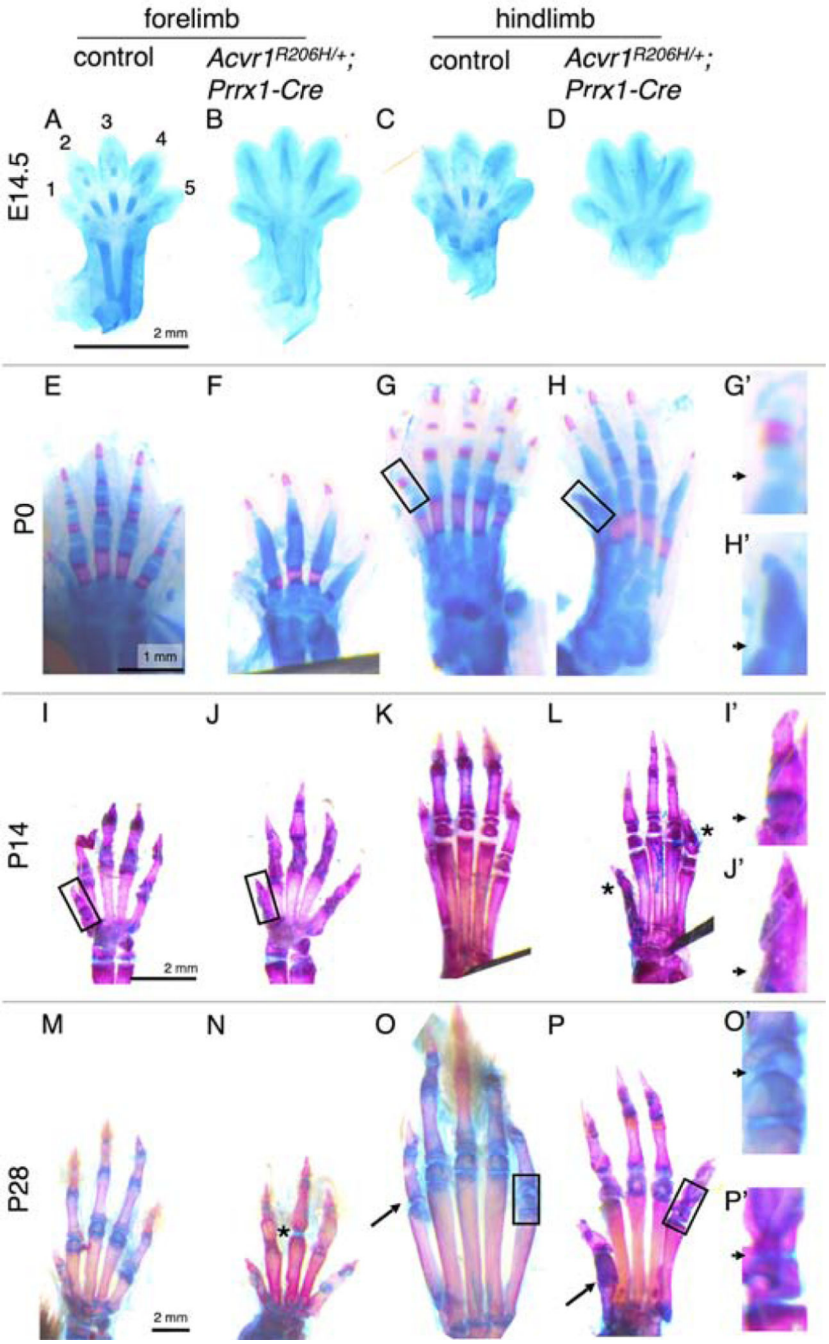

Figure 1. Acvr1 R206H delays and disrupts digit development in a mouse model of FOP.

Digits of forelimbs and hindlimbs of *Acvr1*$^{R206H/+}$;*Prrx1-Cre* and control littermate mice were stained to detect cartilage (Alcian blue) and mineralized bone (Alizarin red) over time from E14.5 to P28. Numbers in (A) indicate digit number from anterior to posterior; all panels, same arrangement. (A-D) At E14.5, mineralization has not yet occurred, and only cartilage is detected. Cartilaginous digit rays are segmented at presumptive joints in controls but not mutants. (E-H) In P0 mutants, Alizarin red staining is limited to digit tips, metacarpals/tarsals of digits 2–5, and first phalanges of digits 3 and 4 of hindlimbs. In

addition, starting at age P0 and continuing through development, phalangeal joints in mutants fail to fully cleave in digits 1 and 5 (insets G' and H', with arrowheads showing expected sites of cleavage). (I-L) In P14 mutants, this failure to cleave in hindlimb digit 1 and 5 (asterisks) and all forelimb digits (J) leads to highly dysmorphic joints (insets I' and J', with arrowheads as in G' and H'). At this stage, medial phalanges of hindlimb digits 2 and 5 and forelimb digits 2 through 5 have failed to form. (M-P) By P28, Alcian blue staining appears reduced in mutants compared to controls in all digit joints, particularly in the area of the growth plates and joints (insets O' and P', with arrowheads as in G' and H'). Asterisk in N denotes example of cartilaginous bridge between phalanges that have failed to separate in forelimb digit 3. Arrows in P indicates the stunted metatarsal of digit 1. Controls were identified by phenotype. All experiments, n≥3.

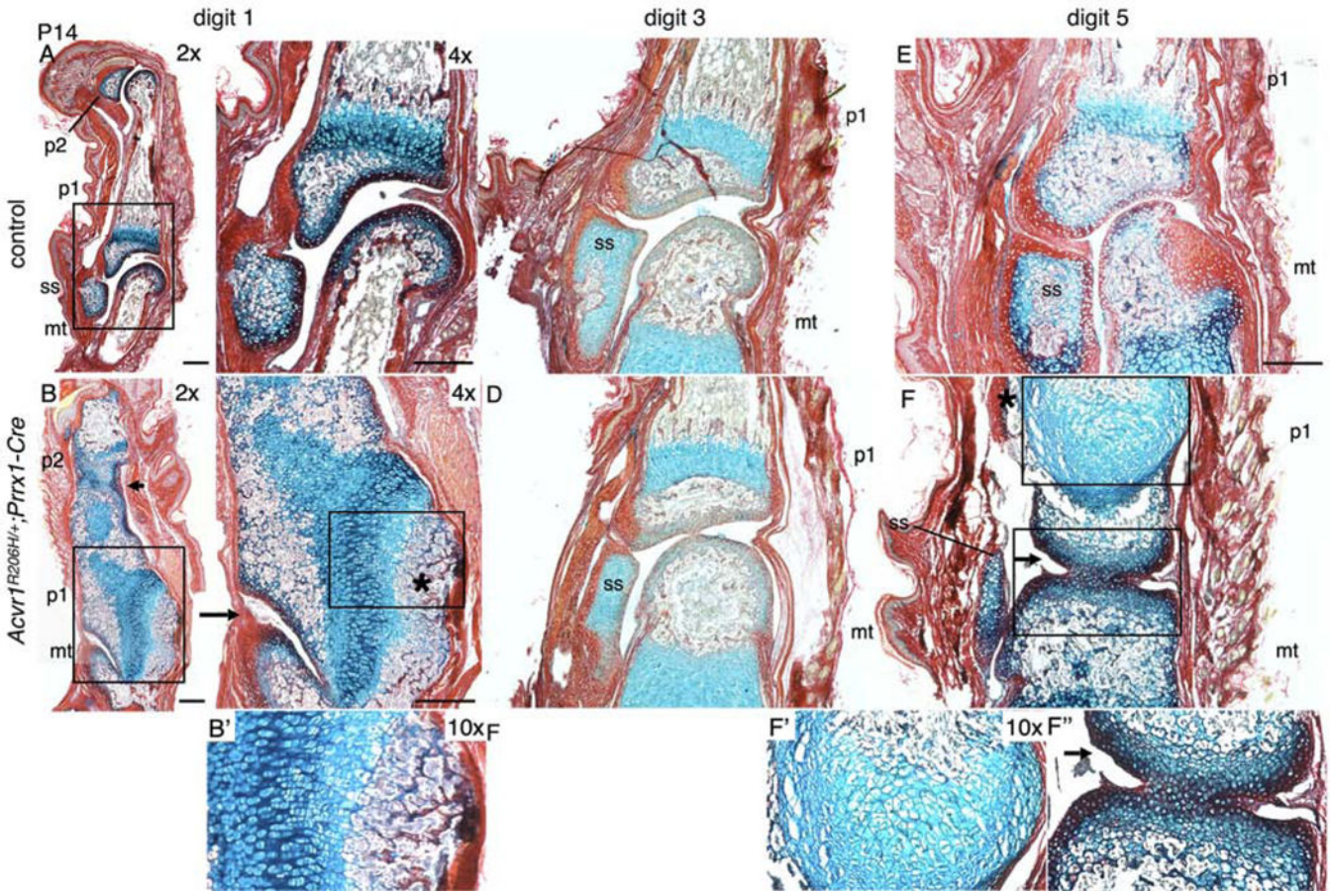

Figure 2. Fused joints and skeletal malformation in *Acvr1*$^{R206H/+}$;*Prrx1-Cre* P14 hindlimb digits.

Sagittal sections of the metatarsophalangeal joints of digits 1 (A, B), 3 (C, D), and 5 (E, F) of P14 mutants and control littermates were stained to detect cartilaginous matrix (Alcian blue) and collagens (picrosirius red). While only minimal defects could be detected in digit 3 in mutants, (C, D), digits 1 and 5 of *Acvr1*$^{R206H/+}$ mice exhibited several anomalous features including dorsal-ventral orientation of apparent endochondral ossification (asterisk, B; B'), ectopic cleavage events (arrow, B), incomplete joint cleavage (arrowheads, B, F, and F") and expanded regions of chondrogenesis (asterisks, B, B', F, and F'). Ventral, left (with digit sesamoids); dorsal, right. mt, metatarsal; p1, phalanx 1; p2, phalanx 2; ss, sesamoid. n≥7, all groups. Controls were identified by phenotype. Scale bars, 250μm.

Figure 3. Malformed joints fail to fully cleave in *Acvr1*$^{R206H/+}$;*Prrx1-Cre* P28 hindlimb digits.
Histological sections of the metatarsophalangeal (MTP) joints of digits 1 (A, B), 3 (C, D), and 5 (E, F) of P28 mutants and control littermates were stained to detect cartilaginous matrix (Alcian blue) and collagens (picrosirius red). (A,B) In digit 1 of mutant mice, endochondral ossification has progressed despite failure to fully cleave at the presumptive MTP joint (arrow, B) and nascent osseous tissue has begun replacing the aberrant growth plate cartilage present at P14 (Fig. 2B), leading to dysmorphic skeletal elements. The metatarsal is also significantly smaller than in controls (mt, B). (C, D) Joints of digit 3 (and

other medial digits) remain minimally affected. (E, F) In digit 5 of mutants, 3/7 mice showed cleavage of the MTP joint (arrow, F; compare with arrow and bracket in E, indicating normal separation between bones) and tissue is disorganized throughout the joint. The morphology of the sesamoid is also altered in mutants. mt, metatarsal; p1, phalanx 1; p2, phalanx 2; ss, sesamoid. n≥7, all groups. Controls were identified by phenotype. Scale bars, 250μm.

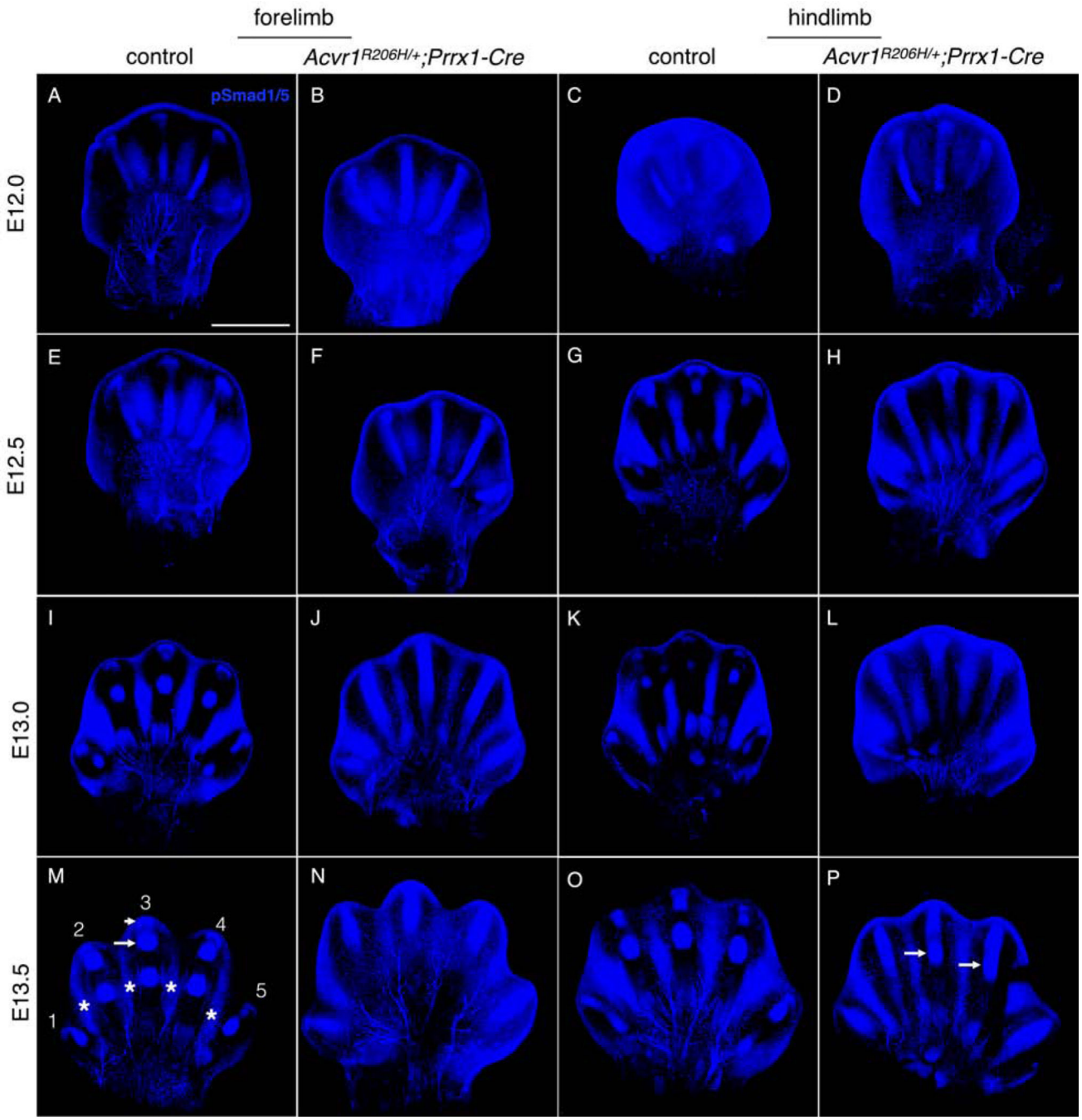

Figure 4. Dysregulated BMP-pSmad1/5 pathway activity throughout the developing *Acvr1*$^{R206H/+}$ digit rays.

Whole-mount immunohistochemistry and confocal imaging detected pSMAD1/5 at E12.0 (A-D), E12.5 (E-H), E13.0 (I-L), and E13.5 (M-P) in forelimbs and hindlimbs of control and *Acvr1*$^{R206H/+}$;*Prrx1-Cre* mice. As indicated in panel M, all panels show digit 1 at left; pSMAD1/5 (blue) is detected in the interdigital tissue (indicated by asterisks) and in the developing skeletal elements (example indicated by arrow) as well as the digit crescent (arrowhead). Arrows in P highlight delayed emergence of discrete zones of BMP signaling in digit rays 3 and 4. All experiments, n≥3. Controls were pooled wild type and single

heterozygotes; no differences were observed among control genotypes. Scale bar panel A, 500 μm.

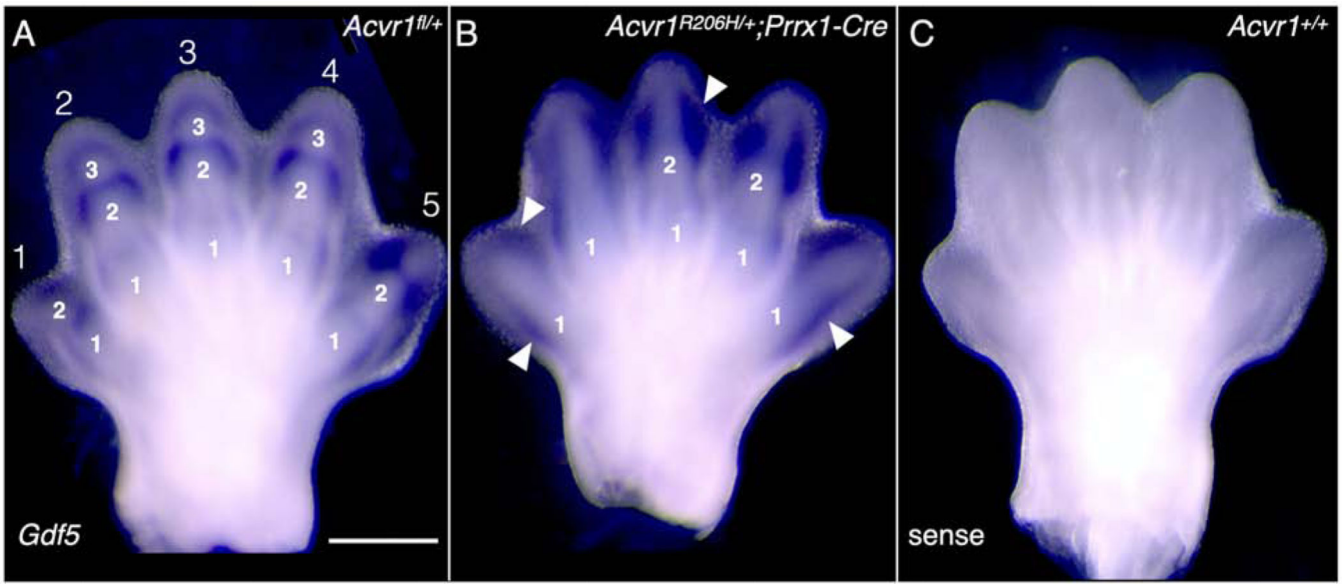

Figure 5. *Gdf5* expression is not appropriately localized to the presumptive joints.

(A) Whole mount *in situ* hybridization of control E14.5 hindlimb digits showed the expected bands of *Gdf5*-expressing cells (dark purple) in the developing digit (n=3). Digits are numbered 1 through 5 with developing phalanges numbered 1, 2, or 3 (proximal to distal; bolded numbers). (B) In contrast, *Gdf5* expression in mutant littermates is at the digit periphery (arrowheads, B; n=2; also see Supplementary Figure S6); each digit shows loss of at least one band of *Gdf5* expression with corresponding reduction in nascent skeletal elements (numbers). (C) Sense probe, negative control. Control mice were pooled from 2 $Acvr1^{fl/+}$ heterozygotes and 1 *Prrx1-Cre* hemizygote; $Acvr1^{fl/+}$ is shown). Scale bar is shown in panel A, 500 μm.